Progress In Electromagnetics Research C, Vol. 33, 171–184, 2012

WCIP APPLIED TO SUBSTRATE INTEGRATED WAVEGUIDE

A. I. Alhzzoury[1, 2, *], N. Raveu[1], O. Pigaglio[1], H. Baudrand[1], and K. Al-Abdullah[3]

[1]University of Toulouse, INPT, UPS, LAPLACE, ENSEEIHT, CNRS 2, Rue Charles Camichel, B.P. 7122, CP 31071 Toulouse Cedex 7, France

[2]Ittihad Private University, Alraka, Syria

[3]Laboratory LMRS, Faculty of Electronic and Electrical Engineering, University of Aleppo, Syria

Abstract—This article presents an efficient method for characterization of substrate integrated passive circuits. The analysis is based on the wave concept formulation and the iterative resolution of a system of two equations between incident and reflected waves. Simulations obtained are compared with analytical references and HFSS simulations. A good agreement is achieved with computation time saving.

1. INTRODUCTION

Substrate integrated waveguide, cavity and filter may be analyzed by full-wave analysis software based on Finite-Difference Time-Domain (FDTD) [1] or Method Of Moments (MOM) [2, 3] and recently with semi-analytical method based on Greens function [4]. All these methods need high memory storage and computation time.

In this paper, the Wave Concept Iterative Procedure (WCIP) method is developed to study substrate integrated structures. The advantage of this method remains in its ease of use due to the absence of test functions; its fast computation time, mainly due to the systematic use of Fast Mode Transform (FMT) and surface mesh use. This method proved its efficiency through several studies of microwave circuits [5–7], coupling between antennas on concentric cylinders [8]....

To validate the proposed approach, several examples of SIW structure are considered. Scattering coefficients obtained with the

Received 27 August 2012, Accepted 7 October 2012, Scheduled 8 October 2012

* Corresponding author: Ahmad Ismail Alhzzoury (ahmad@laplace.univ-tlse.fr).

WCIP are successfully compared to published results, measurements and simulations obtained from other methods.

2. THEORY

The iterative method replaces the transverse fields concerned in the traditional numerical algorithm with the transverse electromagnetic waves and its whole procedure crosses the spatial domain and the spectral domain [9].

The iterative process is constructed via a multiple reflection procedure, which contains three main parts: source excitations, the spatial-domain and the spectral domain scattering [10]. The connection between the spatial domain and spectral domain is carried out via the Fast Modal Transform (FMT) and its inverse (FMT^{-1}). A legible description of the process is illustrated in Figure 1.

Where:

$\vec{\mathbf{A}}$ denotes the emitted waves while $\vec{\mathbf{B}}$ denotes reflected waves seen from the interface.

$\vec{\mathbf{A}_0}$ denotes the incident source waves.

$\hat{\mathbf{S}}$ is the scattering operator which is defined in the spatial domain and accounts for the boundary conditions.

$\hat{\mathbf{\Gamma}}$ is the scattering operator which is defined in the modal domain and accounts for homogeneous media representation.

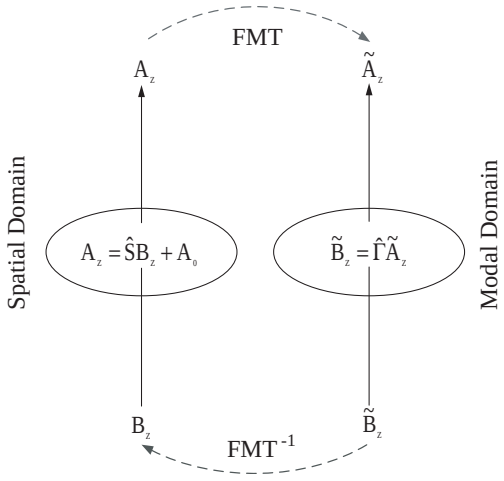

Figure 1. WCIP iterative process.

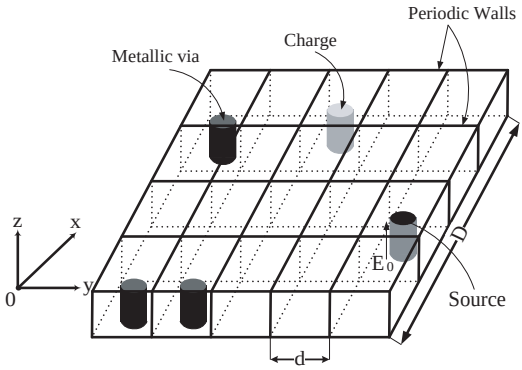

Figure 2. Substrate integrated circuit example.

2.1. Analysis of Integrated Structure with WCIP [10]

This method has been modified to study SIW (Substrate Integrated Waveguide) [10]. An example is presented in Figure 2.

The electric scattered field in such structure is considered linearly polarized along z axis. In the presented formulation, volumic waves are deduced from fields $\mathbf{E}_z(i,j)$ and $\mathbf{J}_z(i,j)$, in each cell through (1).

$$\begin{cases} \mathbf{A}_z(i,j) = \frac{1}{2\sqrt{\mathbf{Z}_0}}(\mathbf{E}_z(i,j) + \ \mathbf{Z}_0\mathbf{J}_z(i,j)), \\ \\ \mathbf{B}_z(i,j) = \frac{1}{2\sqrt{\mathbf{Z}_0}}(\mathbf{E}_z(i,j) - \ \mathbf{Z}_0\mathbf{J}_z(i,j)). \end{cases} \tag{1}$$

$\mathbf{Z}_0$ is an arbitrary impedance.

$\mathbf{E}_z$ is the electric field along z axis; $\mathbf{J}_z$ is the volumic current along z axis; i, j denote the cell position in the SIW mesh.

Fields are defined at the position of the via hole in each cell, through a projection on a H normalized function indicating the via hole position in the cell [10].

2.2. The Scattering Operator in Spatial Domain

At each step of the iterative process, A_z are generated by B_z thanks to (2):

$$\mathbf{A}_z = \hat{\mathbf{S}}\mathbf{B}_z + \mathbf{A}_0 \tag{2}$$

where $\hat{\mathbf{S}}$ takes into account the boundary conditions in the spatial domain.

The SIW can be constructed from four elementary cells represented in Figure 2. They all present different boundary conditions that are detailed in this part:

- The first one presents a metallic via hole in its center, therefore $S_{ij} = -1$.
- The second one is empty, therefore $S_{ij} = 1$.
- The third one presents a current source on the centered via hole $S_{ij} = 0$ (for $\mathbf{Z}_0 = \mathbf{Z}_{0S}$, $\mathbf{Z}_{0S}$ being the source internal impedance).
- The fourth one presents an absorbing via in its center, therefore $S_{ij} = 0$.

2.3. The Scattering Operator in Modal Domain

The substrate height h is considered small enough to have only a surface TM mode within $z \in [0, h]$, the modal scattering coefficient is deduced from the modal impedance operator $\hat{\mathbf{Z}}$ defined in (3)

$$\tilde{E}_z = \hat{\mathbf{Z}}\tilde{J}_z \tag{3}$$

where: $\tilde{J}_z$ and $\tilde{E}_z$ are modal amplitude of $\mathbf{J}_z$ and $\mathbf{E}_z$ respectively.

$$\hat{\mathbf{Z}} = \sum_{\alpha\beta} |\mathbf{F}_{\alpha\beta}\rangle \mathbf{Z}_{\alpha\beta} \langle \mathbf{F}_{\alpha\beta}\,| \tag{4}$$

with: $\boldsymbol{\alpha}$ and $\boldsymbol{\beta}$ index of the basis function of the circuit.

$\mathbf{F}_{\alpha\beta}$ the modal basis function of the circuit defined in Figure 2. Its expression is detailed in (5).

$$\mathbf{F}_{\alpha\beta} = \frac{1}{\mathbf{D}} e^{\alpha x} e^{\beta y}. \tag{5}$$

with :

$$\alpha = \frac{2\pi p}{\mathbf{D}} \quad \text{and} \quad \beta = \frac{2\pi q}{\mathbf{D}} \qquad \text{where} \quad p, q \in \mathbb{Z}$$

$\mathbf{Z}_{\alpha\beta}$ is the modal impedance related to the $\alpha\beta$ mode. Its definition is expressed in (6):

$$Z_{\alpha\beta} = \sum_{n,m} \frac{j\omega\mu_0 \left| \left\langle \frac{1}{\sqrt{S}} H(x,y) | f_{\alpha\beta,mn} \right\rangle \right|^2}{k_0^2 \varepsilon_r - \alpha_m^2 - \beta_n^2} \tag{6}$$

with $\mathbf{H}$ the normalized function indicating the via hole position in the cell; $\mathbf{S}$ being the surface of the via; $\mathbf{H(x, y)}$ is equal to 1 if the point (x, y) is on the via, and zero elsewhere; $\boldsymbol{\mu}_0$ denotes the permeability of the substrate; $\boldsymbol{\omega}$ the pulsation; $f_{\alpha\beta,mn}$ the modal basis function on the elementary cell bounded by periodic walls detailed in (7).

$$f_{\alpha\beta,mn} = \frac{1}{d} e^{j\alpha_m x} e^{j\beta_n y} \tag{7}$$

with:

$$\alpha_m = \left(\alpha + \frac{2\pi m}{\mathbf{d}}\right) \quad \text{and} \quad \beta_n = \left(\beta + \frac{2\pi n}{\mathbf{d}}\right) \quad \text{where} \quad m, n \in \mathbb{Z}$$

According to waves definition, the modal scattering coefficient is (8).

$$\Gamma_{\alpha\beta} = \frac{Z_{\alpha\beta} - Z_0}{Z_{\alpha\beta} + Z_0} \tag{8}$$

The related equation is therefore (9).

$$\tilde{B}_z = \hat{\Gamma}\tilde{A}_z \tag{9}$$

with:

$$\hat{\Gamma} = \sum_{\alpha\beta} |F_{\alpha\beta}\rangle \Gamma_{\alpha\beta} \langle F_{\alpha\beta}| \tag{10}$$

$\tilde{A}_z$ and $\tilde{B}_z$ modal amplitudes of waves.

The operator $\hat{\Gamma}$: traduces the response of the external environment between the incident waves and reflected waves in the modal domain.

3. APPLICATIONS

The method accuracy is verified by examination of analytical test cases and published references [4, 11].

3.1. TEM Propagation in SIW

The structure represented in Figure 3, is bounded by periodic walls on $y = 0$ and $y = d$, and magnetic walls on $x = 0$ and $x = l_2$. The source is represented on 1 mesh. The radius and spacing (center to center) vias are respectively 0.083 mm and 0.46 mm, using 10 metallic vias is sufficient to achieved prefect metallic condition. The substrate relative permittivity is of 4.3 and its thickness is 3.2 mm. The distance l_1 from the sources to the metallic wall (represented by vias) is 211.14 mm, the length l_2 is 225.4 mm, In order to validate the iterative method, the wave number is compared to its theoretical value at 9.8 GHz.

The theoretical value of the wavenumber is 425.62 rad $\cdot$ m^{-1} at 9.8 GHz according to (11)

$$k = k_0\sqrt{\varepsilon_r} = \frac{2\pi}{\lambda} \tag{11}$$

At 9.8 GHz, 28 periods represent a length of 207 mm, as presented in Figure 4, therefore λ is 14.78 mm. The simulated wavenumber is therefore of 424.84 rad $\cdot$ m^{-1}. The simulation error on the wavenumber obtained with WCIP is 0.18%. The FEM simulation leads to a

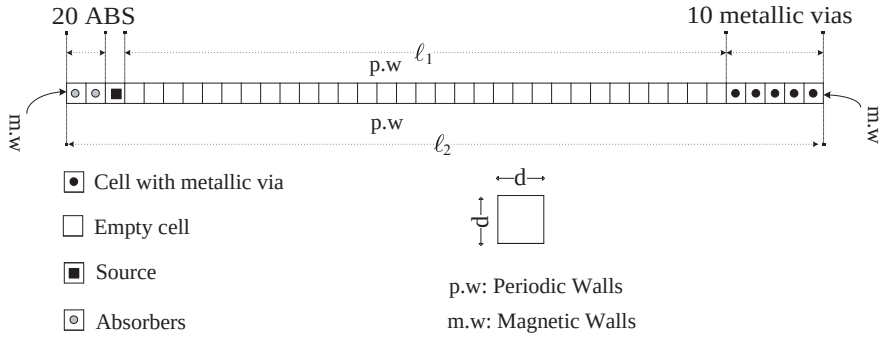

Figure 3. SIW for TEM propagation.

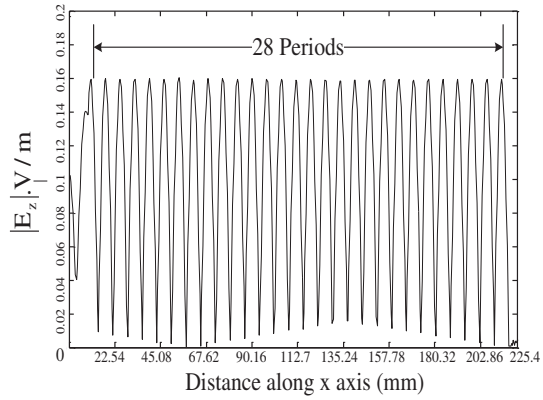

Figure 4. Electric field E at 9.8 GHz along x for $y = d/2$.

368.94 rad $\cdot$ m^{-1} in the same conditions. The simulation error for FEM on the wavenumber is 13.16%.

The simulation time with the WCIP is 16 s against 1 min 1.4 s for the FEM software for one frequency point simulation. (CPU: Intel Core 2 Due E6550@2.33 GHz, RAM: 4Go).

3.2. $\mathbf{TE}_{10}$ Propagation in SIW

Sources are represented on 20 meshes with sinusoidal variation along y axis to represent the $\mathbf{TE}_{10}$ mode. The structure is shown in Figure 5. The structure is bounded by periodic walls at $y = 0$ and $y = w$, and magnetic walls at $x = 0$ and $x = l_2$.

Dimensions are identical to the previous case.

The structure width w is 13.8 mm, the length l_2 is 225.4 mm. The

waveguide drowned in this structure width is 9.66 mm. This width is compared to the effective width W_{eff} evaluated with (12) through simulation of k.

$$W_{eff} = \frac{\pi}{\sqrt{k_0^2 \varepsilon_r - k^2}} \tag{12}$$

with:

$$k = \frac{2\pi}{\lambda_g}$$

k is computed through the standing wave period observation.

At 12 GHz, 26 periods represent a length of 201.48 mm as presented in Figure 6, therefore λ_g is 15.4985 mm. So the effective width W_{eff} is 9.5926 mm. The relative error obtained with WCIP is 0.69%. The FEM simulation achieved with HFSS leads to an effective width of 10 mm in the same conditions. The simulation error for FEM on the wavenumber is 3.5%.

The simulation time with the WCIP is of 8.8 s against 1 hour 28 min for the FEM software for one frequency point simulation. Computation time in FEM simulation is due to the important number of metallic via 1180 compared to 10 in previous case.

3.3. SIW Coupled Cavities [11]

The internal coupling of two coupled SIW cavities is studied. The dimensions of the coupled cavities, as shown in Figure 7, are $p = 1$ mm, $d = 0.75$ mm, $w_1 = l = 26$ mm, $w_2 = 4$ mm. The thickness of the substrate is 0.5 mm, its relative permittivity is $\varepsilon_r = 2.65$. The evanescent waveguide section has a constant length of $w_z = 4$ mm.

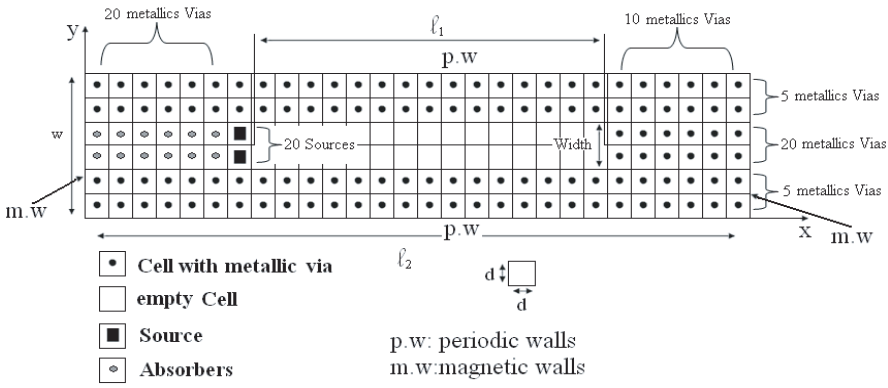

Figure 5. SIW for TE_{10} propagation.

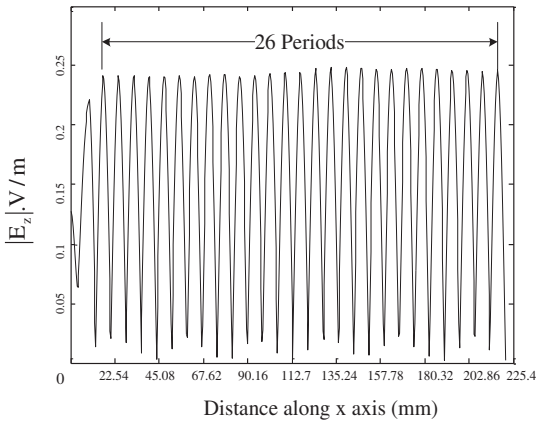

Figure 6. Electric field E at 12 GHz along x for $y = w/2$.

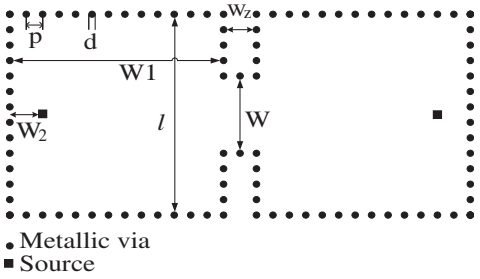

Figure 7. SIW coupled cavities.

WCIP results are compared to HFSS for coaxial feeds positioned according to Figure 7 dimensions. Good agreement is found between WCIP and HFSS results as presented in Figure 8.

The coupling coefficient between cavities is given by (13) [4].

$$k = M\frac{(f_{02} - f_{01})}{\sqrt{f_{02} \cdot f_{01}}} \tag{13}$$

with M the generalized coupling matrix [4], its value is 0.9371. f_{01} and f_{02} are the cut off frequencies at -20 dB. Coupling coefficient is presented in Figure 9 for several evanescent waveguide section widths w. Results obtained are compared with FEM ones. The relative error reported in Table 1 is lower than 4.4%.

The simulation time with the WCIP is 5.1 s for one frequency point simulation against 4.8 min for the FEM software (HFSS).

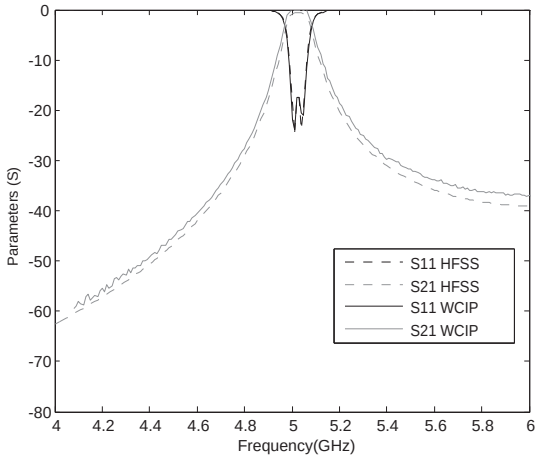

Figure 8. SIW coupled cavities ($w = 10\,\text{mm}$).

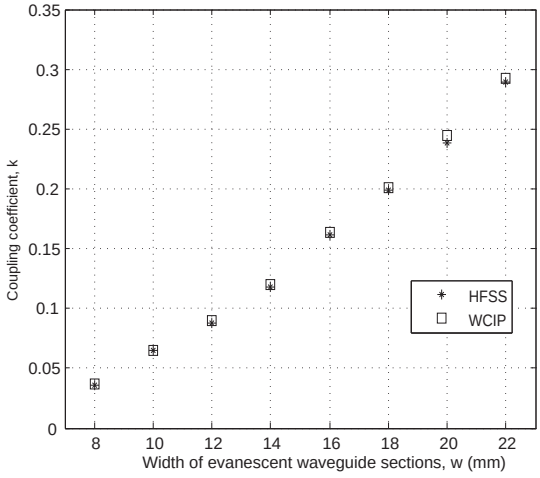

Figure 9. Coupling coefficients, k for several evanescent waveguide section widths.

Table 1. Relative error between WCIP and HFSS of Figure 9.

W (mm)	8	10	12	14	16	18	20	22
Error (%)	4.4	0.7	2.2	1.6	1.8	0.9	2.8	1

3.4. SIW Filter

The proposed SIW bandpass filter was fabricated on a single-layer Arlon AD255A (tm) substrate with a permittivity of 2.55, dielectric

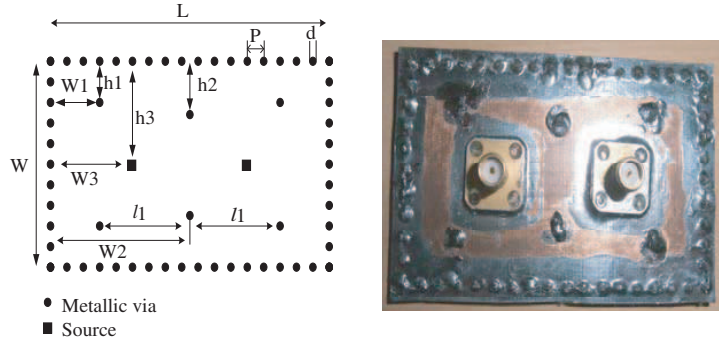

Figure 10. SIW filter.

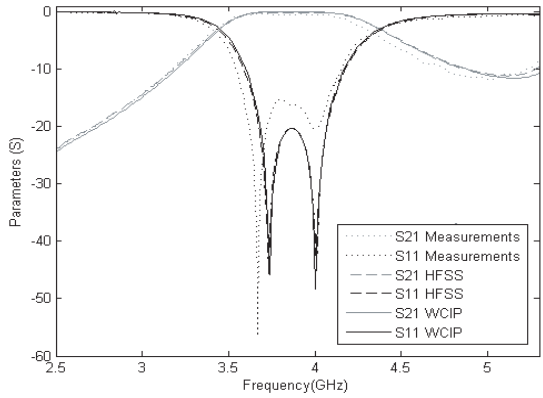

Figure 11. SIW filter with coaxial feed [12].

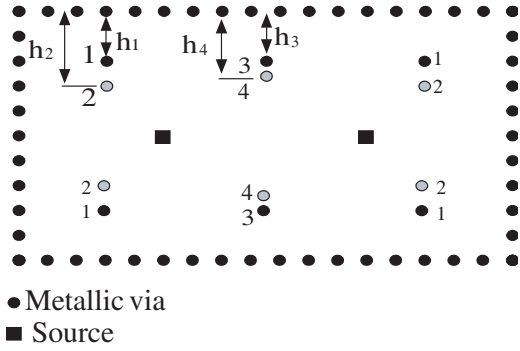

Figure 12. SIW filter.

Table 2. Filter center frequency and relative bandwidth.

Circuit 1	fc1	3.79 GHz	Δfc1	22.8%
Circuit 2	fc2	3.88 GHz	Δfc2	16.1%
Circuit 3	fc3	4.15 GHz	Δfc3	21.45%

loss tangent 0.0015 and height of 1.524 mm. The bandpass filter is of order 2 and has a center frequency of 3.8 GHz. The bandwidth is off 19% with a ripple of 0.05 dB. The metallized via-holes have a diameter d of 1.25 mm and a center-to-center pitch p of 4 mm. Two resonators and three inverters compose the bandpass filter. The resonator length l_1 is 22 mm. Perfectly metallic walls are replaced by vias that must meet equivalent boundary conditions. The SIW Filter is symmetric its dimensions are $L = 68$ mm, $W = 40$ mm, $W_1 = 12$ mm, $W_2 = 34$ mm, $W_3 = 20$ mm, $h_1 = 8$ mm, $h_2 = 10$ mm and $h_3 = 20$ mm. A picture and scheme are presented in Figure 10.

Results 12 obtained by the WCIP are in very good agreement with other numerical methods FEM (obtained with HFSS) and measurements (Figure 11). Sensitivity studies were performed thanks to the WCIP to reduce the number of via [12]. The simulation time with the WCIP is 1.86 s for one frequency point simulation against 37 s for the FEM software. The number of metallic via in WCIP and FEM is 60.

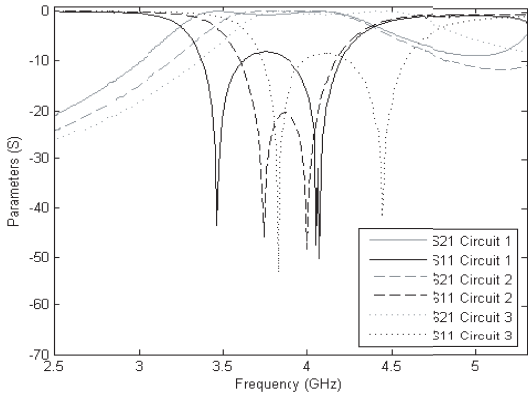

Figure 13. Parameters S.

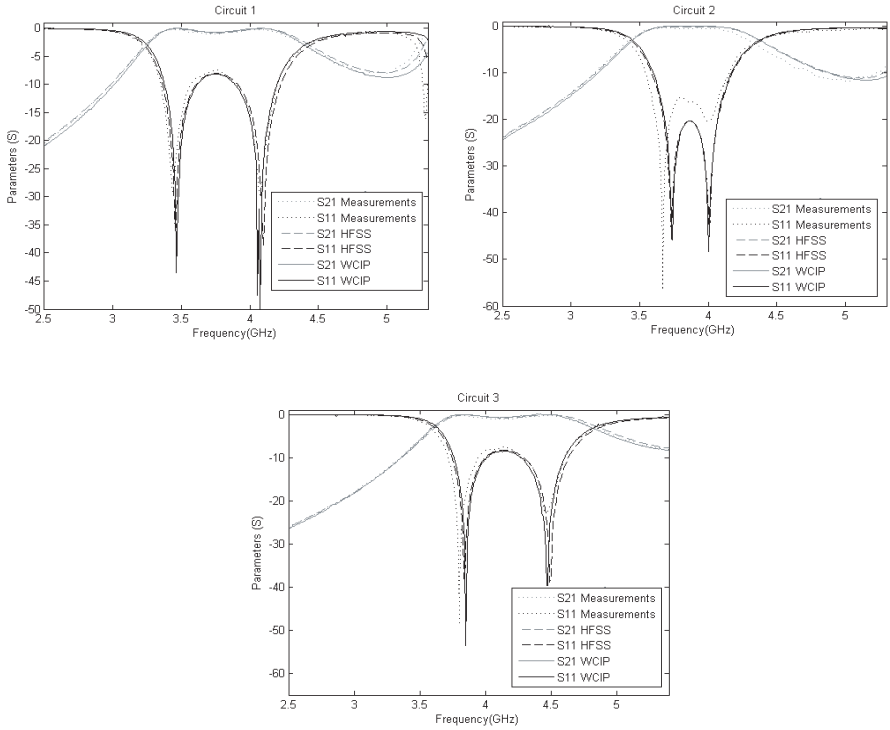

Figure 14. SIW filter response of Circuit 1, Circuit 2 and Circuit 3.

3.5. Reconfigurable SIW Filter

In the previous design, inverters are conditioned by aperture width, thus by the position of via bounding their dimensions. Changing these apertures with active devices allow tunable filters design. The number of vias is increased to change external and internal aperture widths only 3 over the 4 filter configurations are interesting. Results are presented for ideal switches in the on state. All dimensions are left unchanged compared to Figure 10, vias positions are indicated in Figure 12. Where $h_1 = 8\,\text{mm}$, $h_2 = 12\,\text{mm}$, $h_3 = 8\,\text{mm}$, $h_4 = 10\,\text{mm}$. In Circuit 1, vias n°1 and 3 are activated, in Circuit 2, vias n°1 and 4 are activated, Circuit 3, vias n°2 and 4 are activated.

Circuits results are presented on Figure 13 which shows a shift of the filter center frequency of order 2 and ripple 0.7 dB and the relative bandpass, with a change in the bandwidth, as reported in the Table 2.

Results obtained by the WCIP are in very good agreement with HFSS and measurements (Figure 14). The simulation time for

Circuit 1, Circuit 2 and Circuit 3 are respectively with the WCIP of 3.07 s, 1.86 s, 13.03 s against 40 s, 37 s, 83 s for HFSS for one frequency point simulation. (CPU: Intel Core 2 Due E6550@2.33 GHz, RAM: 4Go).

4. CONCLUSIONS

WCIP method seems to be an efficient method for SIW study. The efficiency of the method has been proved through the analysis of test cases on SIW structures. The computation time remains small compared to FEM software (HFSS). A good agreement is achieved between our results, theory and measurements. Moreover this method aims at simulating large number of via holes and may therefore be used for a complete SIW chain. Its performance in computation time compared to HFSS is obvious when the number of via gets important.

REFERENCES

1. Simpson, J. J., A. Taflove, J. A. Mix, and H. Heck, "Computational and experimental study of a microwave electromagnetic bandgap structure with wave guiding defect for potential use as a bandpass wireless interconnect," *IEEE Microwave and Wireless Components Letters*, Vol. 14, 343–345, 2004.
2. Yang, H.-Y. D., R. Kin, and D. R. Jackson, "Design consideration for modeless integrated circuit substrates using planar periodic patches," *IEEE Transactions on Microwave Theory and Techniques*, Vol. 48, 2233–2239, 2000.
3. Chow, Y. L. and W. Che, "Successive SIW (substrate integrated waveguides) types for width reductions by physical reasoning and formulas by analytical (use of) MoM," *IEEE Microwave and Millimetre Wave Technology*, 1746–1749, 2008.
4. Macchiarella, G. and S. Tamiazzo, "Design techniques for dual-passband filters," *IEEE Transactions on Microwave Theory and Techniques*, Vol, 53, No. 11, 3265–3271, Nov. 2005.
5. Zairi, H., H. Baudrand, A. Gharsallah, and A. Hafidh Gharbi, "An efficient iterative method for analysis of a substrate integrated waveguide structures," *Microwave and Optical Technology Letters*, Vol, 52, No. 1, Jan. 2010.
6. Trabelsi, H., A. Gharsallah, and H. Baudrand, "Analysis of microwave circuits including lumped elements based on the iterative method," *International Journal of RF and Microwave Computer-Aided Engineering*, Vol. 13, 269–275, 2003.

7. Zaabat, M., H. Amri, and H. Baudrand, "Rigorous approach of the planar circuit," *The Online Journal on Electronics and Electrical Engineering (OJEEE)*, Vol, 2, 255–258, 2009.
8. Raveu, N., T. P. Vuong, I. Terrasse, G.-P. Piau, G. Fontgalland, and H. Baudrand, "Wave concept iterative procedure applied to cylinders," *IEEE Proceedings on Microwave, Antennas and Propagation*, Vol. 151, No. 5, 409–416, Oct. 2004.
9. Wang, Y. Y., Y. J. Xie, and H. Feng, "Analysis of cylindrically conformal microstrip structures using an iterative method," *Progress In Electromagnetics Research*, Vol. 87, 215–231, 2008.
10. Raveu, N. and H. Baudrand, "Metallic EBG characterization with the WCIP," *IEEE Antennas and Propagation Symposium, APS-URSI*, Charlestown, 2009.
11. Chen, X., W. Hong, T. Cui, J. Chen, and K. Wu, "Substrate integrated waveguide (SIW) linear phase filte," *IEEE Microwave and Wireless Components Letters*, Vol. 15, No. 11, 787–789, Nov. 2005.
12. Alhzzoury, A. I., N. Raveu, G. Prigent, O. Pigaglio, H. Baudrand, and K. Al-Abdullah, "Substrate integrated waveguide filter design with wave concept iterative procedure," *Microwave and Optical Technology Letters*, Vol. 53, No. 12, 2939–2942, Dec. 2011.